

PAPER • OPEN ACCESS

## Investigating the Effects of Nano Ceramics based Pack Cementation Coatings on Properties of some Biomedical Ti Alloys

To cite this article: Zainab Zuhair Ali and Fatimah J Al-Hasani 2021 *IOP Conf. Ser.: Mater. Sci. Eng.* **1094** 012167

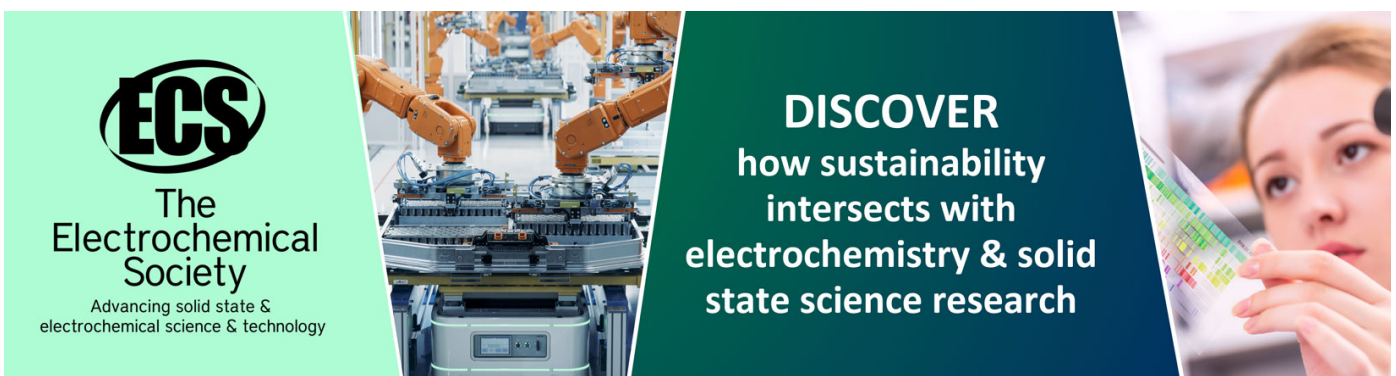
View the [article online](#) for updates and enhancements.

You may also like

- [Ni-Al phase transformation of dual layer coating prepared by pack cementation and electrodeposition](#)  
A Afandi, E Sugiarti, R Ekaputra et al.

- [Influence of process parameters and rare earth content on the properties of niobium carbide coatings synthesized by pack cementation](#)  
Shuai Li, Ruike Wang, Zongying You et al.

- [Combined niobizing and plasma nitriding of AISI 430 stainless steel](#)  
N jalalian Karazmoudeh, M Soltanieh and M Heydarzadeh Sohi



**ECS**  
The  
Electrochemical  
Society  
Advancing solid state &  
electrochemical science & technology

**DISCOVER**  
how sustainability  
intersects with  
electrochemistry & solid  
state science research

# Investigating the Effects of Nano Ceramics based Pack Cementation Coatings on Properties of some Biomedical Ti Alloys

**Zainab Zuhair Ali and Fatimah J Al-Hasani**

Materials Engineering Department, University of Technology, Baghdad, Iraq

E-mail: 130141@uotechnology.edu.iq

**Abstract.** Titanium has a unique ability to bind with bone and living tissue, making it an ideal material for orthopedic implants such as knee and hip replacements. The objective is focused on studying the influence of Nano ceramic powder (70%ZrO<sub>2</sub> with Y<sub>2</sub>O<sub>3</sub>) on different base titanium alloys produced by powder technology technique (Ti-pure, Ti-45%Ni, Ti-10%Co, and Ti-30%Ta) with pretreated surface of implant samples. From XRD patterns, there was no indication that other phases contain any of the diffraction patterns present in samples after (ZrO<sub>2</sub> and Y<sub>2</sub>O<sub>3</sub>) deposition. The microstructure observation of all samples showed that both Nano zirconia and yttria were distributed in samples surface and covered, which produced a high modification in morphology of surface. There was considerable increase in hardness value after pack cementation process. It is evident that the porosity percent of the samples after Nano ceramic deposition largely decreased. The results showed that using chemical pre surface treatments and powder technology method was useful to gain adhere and homogenous deposition layer.

**Keywords.** Biomedical Ti alloys, Nano ZrO<sub>2</sub> and Y<sub>2</sub>O<sub>3</sub>, Pack cementation process, Porosity percentage.

## 1. Introduction

Due to desirable properties of titanium and titanium alloys, such as relatively low modulus, strong fatigue strength, formability, machinability, corrosion resistance, and biocompatibility, are highly utilized in biomedical devices and implant, particularly like in the use of cardiac and cardiovascular and in replacements of hard tissue [1,2]. Hard tissues are damaged most because of aging, accidents, and other causes. In the response of the biological environment to artificial medical devices, the surface of the material plays an extremely important role [3]. Ti-Ni alloys can be used both for hard and soft tissues. Mechanical characteristics of Ti-Ni depend on its state of phase at a certain temperature [4, 5]. For several years, Ti-Co alloys have been used extensively in dentistry and medicine as implant alloys. The Ti-based cobalt addition alloys therefore exhibit greater strength and have lower melting temperatures, which can mitigate many casting problems. Adding cobalt increases titanium corrosion resistance and its mechanical properties. Broad applications were also found in the ternary (Ti-Co)-based alloys [6, 7]. The Ti-30 %Ta alloy has earned comprehensive application in the biomedical materials. In this research, titanium alloys



with Ta will be considered because it offers significantly enhanced mechanical properties, including fracture strength and workability, showing enhancement of both pure Titanium and pure Tantalum. Furthermore, it has been shown that the use of 30 % Ta has a powerful impact on both the young modulus and tensile properties of binary Ti-Ta alloys [8, 9]. Zirconia is an oxide which has a high tensile strength, high hardness and corrosion resistance [10]. During phase modification at high temperatures in pure form, it undergoes a significant volume change; thus, a dopant oxide like  $Y_2O_3$  is utilized to stabilize the high-temperature (cubic) phase [11]. For bone implantation, we used  $Y_2O_3$  as a dopant to have zirconia. Zirconia formed in this way is referred to as zirconia that is partially stabilized.

Nano-yttria-stabilized zirconia (n-YSZ) is a ceramic which has been scrutinized extensively in past years. The response time is shortened by particles with a smaller grain size and a higher specific surface. Higher catalytic activity is also induced by the larger surface area. The properties of N-YSZ are due to the large fraction of atoms inside the region of the interface [12, 13]. **F. Al-Hassani (2019)** studied the effect of cobalt percentage on the corrosion rate of sintered titanium dental implants. The goal of this work is to study how Co addition to Ti influences the corrosion behavior of dental alloys. The raw materials used were pure titanium powder and pure cobalt powder. The amount of  $Ti_2Co$  phase slightly increases with increasing cobalt content. The porosity percentage and corrosion decrease with increasing cobalt percentage [14].

**G. Marenzi et al. (2019)** investigated the effect of different surface treatments on titanium dental Implant micro-morphology, in contrast, sandblasted implants could cause potential risks of surface contamination because of the presence of blasting particles remnants. The acid-etched surfaces were characterized by the presence of deeper valleys and higher peaks than the sandblasted surfaces. For this reason, acid-etched surfaces can be more easily damaged by the stress produced by the peri-implant bone during surgical implant placement [15]. **F. Al-Hassani (2020)** examined the effect of ultrasonic assisted zirconia coated Cp – Ti alloys on dental implantation. The deposition of zirconia by ultrasonic waves has been made for pure Titanium alloys to minimize the ions of Ti released from implant surface when inserted inside the body. The result was observed with slight decrease in porosity due to the deposition of zirconia. The hardness results showed that the average value of sample increased after deposition. The surface roughness after zirconia deposition treatment decreased, due to the Nano powder filling the surface porosity which leads to reduction in surface roughness which creates stable surface and forms strong titanium oxide layer which in turn inhabits the ion release [16]. **J. Maminskas et al. (2020)** explored novel yttria-stabilized zirconium oxide and lithium disilicate coatings on titanium alloy substrate for implant abutments and biomedical application. The study aimed to create novel bioceramic coatings on a titanium alloy. The deposition of 3YSZ and LS2 coatings changed the physicochemical properties of the Ti. Both coatings were biocompatible, while Ti-3YSZ demonstrated the most significant cell area and the significantly highest, focal adhesions (FAs) per cell after 24 h. Thus, Ti-3YSZ and Ti-LS2 surfaces might be promising for biomedical applications [17].

The main purpose of that research is using pack cementation as Nano ceramic deposition process resulting in formation of Nano zirconia and yttria layer on the surface to enhance the biomedical titanium alloys used as implant in the body, [18-19].

## 2. Methods and materials

### 2.1. Sample preparation

The first step of the experimental work is the preparation of the four master sample (Ti-pure), (Ti-50%Ni), (Ti-10%Co) and (Ti-30%Ta) using powder technology technique. The elemental powders were used to prepare the master alloy were titanium, nickel, cobalt and tantalum powders. Tables (1) illustrates the properties of powders.

**Table 1.** Properties of powders.

Element	Color	Shape	Mesh	Radius
Ti	Gray	Spherical	200	70 $\mu$
Co	Black	Spherical	200	30 $\mu$
Ni	Silver	Spherical	200	50 $\mu$
Ta	Gray	Spherical	200	45 $\mu$

### 2.2. Ti alloys preparation

The metal powders were weighted by a sensitive balance where the total weight of all specimens is 5 gm. Then powders were mixed in a ball mill for 15 min at 70 rpm speed for each sample. The compaction process of powder of each sample was done by the hydraulic press machine in which powders were pressed under pressure of 7 ton for 10 min, and then the samples with the same diameter of 15 mm and 5 mm height for each type of alloys were produced. The sintering process was done by CVD quartz tube furnace at temperature around 1000 °C for 3:30 h under vacuum (argon gas) to prevent oxidation of samples. Table (2) displays the groups of sample alloys.

**Table 2.** The groups of sample alloys.

Alloy	Group before coating	Group after coating
Ti-pure	P	P1
Ti-45%Ni	N	N1
Ti-10%Co	C	C1
Ti-30%Ta	T	T1

### 2.3. Pretreatment surface

The ultrasonic pre-surface treatment involved cleaning the surface from all dirt and impurities before chemical treatment to get a suitable clean surface for one hour then they were removed and dried. After that, the samples were ready for acid and alkaline treatment, used for removing both of contamination and oxide in order to have clean and good surface finishes. The samples were immersed in HCl acid with concentration of 0.5 mM for four hours at 40C. Then the samples were immersed again in NaOH with concentration of 10 mM for 24 hours at 60C. After this step, the samples were ready for the pack cementation process.

### 2.4. Pack cementation process

The elemental powders used in this process are zirconia ( $ZrO_2$ ), yttria ( $Y_2O_3$ ) and sodium chloride (NaCl), with percentage of powders being 95% ( $ZrO_2$ ) with ( $Y_2O_3$ ) and 5% (NaCl), and the total weight of total deposition powders is 50gm. Then the powders were mixed for 30 min, to obtain a homogeneous distribution of the metal powders and to have very good mixing between elements deposition. Finally, alumina crucible is filled by the produced powder and master samples. The process was done by utilizing CVD quartz tube furnace at temperature of (1000) °C for (3:30) h under controlled atmosphere (argon gas).

### 2.5. Characterization of Samples

The second step is the characterization of samples by a variety of tests conducted in order to get various properties of samples. The tests conducted were (Scanning electron microscope (SEM), Porosity Test, Surface roughness investigation, hardness test and X-ray Diffraction (XRD)) in order to verify the effect of different additions on the titanium behavior in general situations.

*2.5.1. Scanning electron microscope (SEM).* Field Emission Scanning Electron Microscope (FESEM) is a kind of electron microscope that illustrates the specimens by scanning in a large-energy emit of electrons in a raster investigate model. The electron connects with atoms that form the specimen manufacture signals that have data around the topography of specimen surface and composition. The test was conducted in Iran by FESEM device type TESCAN (Czech Republic).

*2.5.2. Porosity Test.* Due to the use of powder metallurgy method to produce samples, the test is necessary to evaluate effect of manufacturing process on the porosity of samples. Porosity measurement was made in the chemistry laboratory, and the porosity percentage was calculated by Archimedes process. This process involves calculating the dry specimens weight, after that the specimens were weighted while they were in basket and dipped in water. Samples were immersed in water for 24 hours, and finally after their surface was cleaned with cloth, the specimens were weighed and the porosity was calculated based on the formula, [20]:

$$\text{Porosity} = ((w_s - w_d) / (w_s - w_n)) * 100\% \quad (1)$$

About:

$w_d$  = dry specimen weight,  $w_s$  = saturated specimen weight, and  $w_n$  = Weight of specimen immersion.

*2.5.3. Surface roughness investigation.* In order to identify the topographic change after surface treatments as well as the amount of roughness that has been produced before and after deposition process surface roughness investigation was done. The test was carried out using Atomic Force Microscope (AFM) located in the Department of Science at the University of Baghdad. The device type was PHYWE/Nano Compact AFM, made in UK.

*2.5.4. hardness test.* Hardness of all samples was obtained by digital hardness analyzer (HBRVS-187.5) which is located at the Materials Inspection Laboratory. The result was an average of 5 points test. The carried load was 1Kg, all hardness values were taken.

*2.5.5. X-ray Diffraction (XRD).* To discover the structure and phase distinguishing of all specimens, XRD test was conducted at Nanotechnology Laboratory- University of Technology by utilizing, Shimadzu diffractometer of X-ray (kind XRD- 6000).

### 3. Results and discussion

#### 3.1. Scanning electron microscope (SEM)

The microstructure of alloy samples (Ti-Pure, Ti-45%Ni, Ti-10%Co and Ti-30%Ta) before deposition of ( $ZrO_2$  and  $Y_2O_3$ ) Nano ceramic powders and after the sintering process (This is Google Translate- where is the verb?!). The surface used high discontinuities and roughness due to the porosity results from type of manufacturing process. It was very good and preferable for preparing the surface to deposition process. By creating initial roughness, the FESEM images of all alloy samples were taken to provide complete view of the topographical changes before and after deposition in all surface area of samples as illustrated in Figure (1) which shows the FESEM image of sample (P). Figure (2) presents the microstructure of sample (N) which has less initial surface roughness than others due to the low size diffraction between raw powders (Ti, Ni). Figure (3) shows the microstructure of sample (C). From these figures, it was noted that the sample had greater initial surface roughness due to the large size differences between raw powders (Ti, Co). Whereas figure (4) shows the microstructures of sample (T). From these figures, it was noticed that the surface had suitable initial roughness results from manufacturing process.

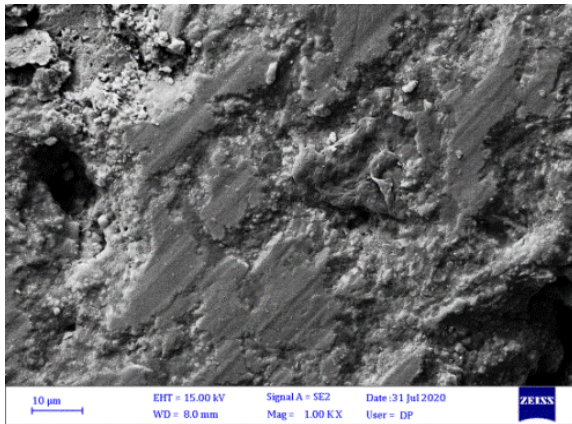


**Figure 1.** SEM image for sample (P).

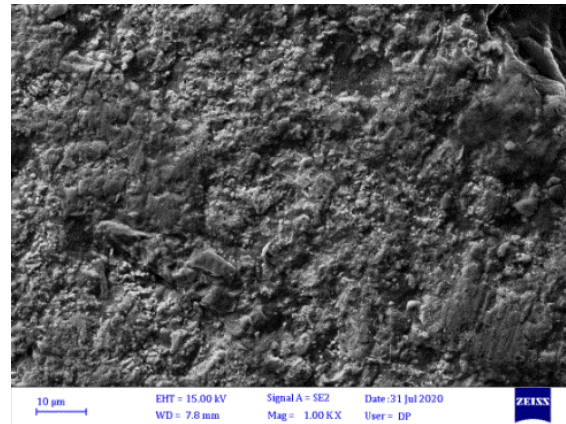


**Figure 2.** SEM image for sample (N).

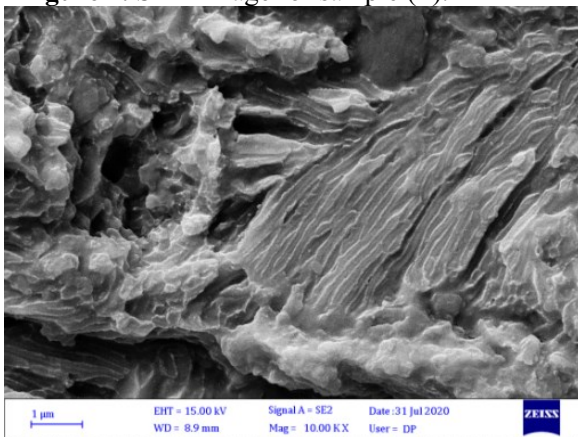


**Figure 3.** SEM image for sample (C).

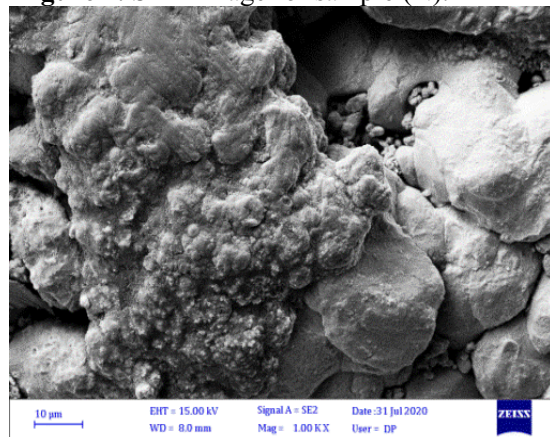


**Figure 4.** SEM image for sample (T).

It was noticed after the samples were deposited by Nano zirconia and yttria using pack cementation that the surface morphology changed completely and had a new surface layer form on the samples. The deposition layer that was observed in Nano scale shown in figures (5, 6, 7, and 8) proved that the Nano ceramic deposition layer was produced on the surface of alloys. Figure (9) shows the microstructure of sample (P1). It is clear that the Nano ceramic material covered all three positions of the same mineral and there was large change in surface texture compared with sample (P). Figure (10) illustrates the formation of new surface texture resulting from depositing of Nano ceramic materials of the surface of sample (N1) and it is important to know there was low morphological changes in sample (N1) compared with others due to the low initial surface roughness in sample (N). While figure (11) for sample (1), shows that the deposition layer occurred and will observe a growth in a certain direction of the deposition layer as a result of a large pore size, high porosity and good surface roughness that led to this distinct deposition behavior. Finally, it was noticed that in the sample (T1) shown in the figure (12), deposits occurred on the surface of the alloy by making change in the surface morphology. Each specimen viewed that Nano zirconia and yttria were produced on the sample surface and fully covered it, resulting in a high modification in the surface morphology. This is due to the initial surface roughness that resulted from manufacturing process (powder technology) and the primary surface treatment (acid –alkaline etching) that was done before the depositing process to prepare the surface for the deposition process. It appears that surface pretreatment and powders manufacturing are the main processes to have both homogeneous and adherent deposition films useful and successful.



**Figure 5.** FE-SEM for sample (P1) in Nano scale.



**Figure 6.** FE-SEM for sample (N1) in Nano scale.



**Figure 7.** FE-SEM for sample (C1) in Nano scale.



**Figure 8.** FE-SEM for sample (T1) in Nano scale.



**Figure 9.** SEM image for sample (P1).



**Figure 10.** SEM image for sample (N1).



**Figure 11.** SEM image for sample (C1).



**Figure 12.** SEM image for sample (T1).

**3.2. Porosity test**

Because of the use of powder metallurgy technique to produce samples, porosity test is substantial to determine the effect of this method on the porosity percentage of samples. The porosity percentage test was also measured by using Archimedes method. The obtained results are represented graphically in figure (13). The chart shows that porosity percentage of sample (C) has a higher value than other alloys type due to the size differences gap between the raw powders. It is evident that the porosity percent of the samples after ( $ZrO_2$  and  $Y_2O_3$ ) deposition largely decreased due to the pack cementation process effect which allows the Nano powder to fill the surface pores and lead to eliminating all surface defects and open porosity. This is clearly shown in figure (14).

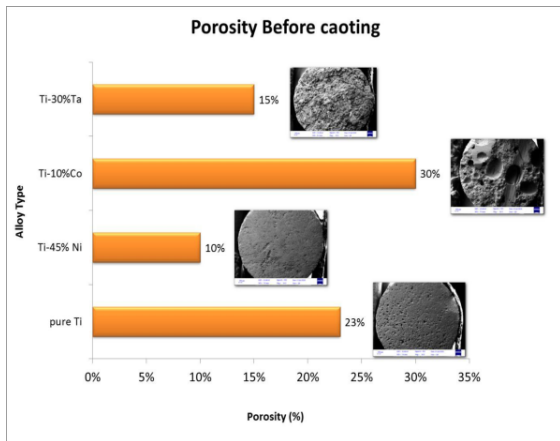


**Figure 13.** Porosity percentage before deposition.

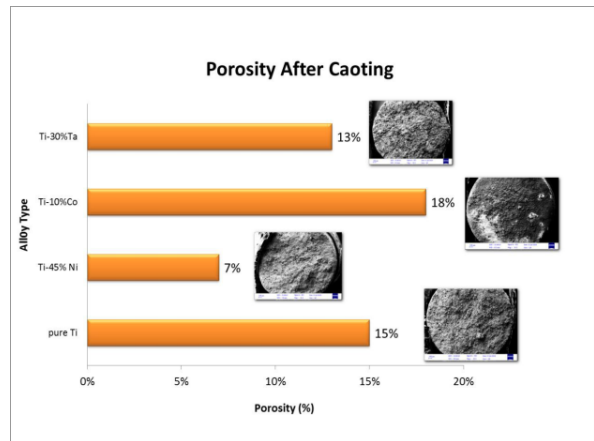


**Figure 14.** Porosity percentage after deposition.

**3.3. Surface roughness investigation**

Roughness of sample surface and its capacity to be fixed in medical bone tissue is considered a very important parameter for medical implants. To raise the roughness of sample surface of the medical implant, many production processes exist. Atomic force microscopy (AFM) revealed the topography of sample surface, in which representations of the three-dimensional outline "topography" of the specimen's surface were found to be of big resolution. This was achieved by scanning the position of the sample with

respect to the tip and recording the height of the probe that corresponds to a constant probe-sample interaction. Figure (15) displays the roughness value of the alloy samples (Ti-Pure, Ti-45%Ni, Ti-10%Co and Ti-30%Ta) before pack cementation deposition with ( $ZrO_2$  and  $Y_2O_3$ ). Representations of the 3-D shape "topography" of the specimen's surface were found to be of big resolution as in Figures (16, 17, 18 and 19). It can be observed that samples (P, N, C and T) which were produced by powder technology process without any surface treatments have roughness of (9.05, 8.8, 10.9 and 15.6nm) respectively.

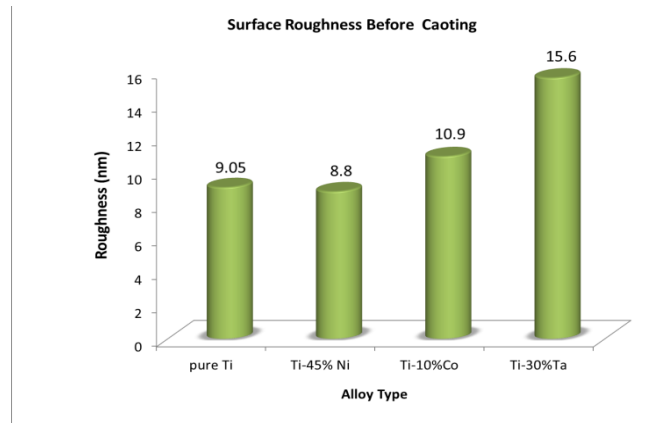


Figure 15. Surface roughness before deposition.

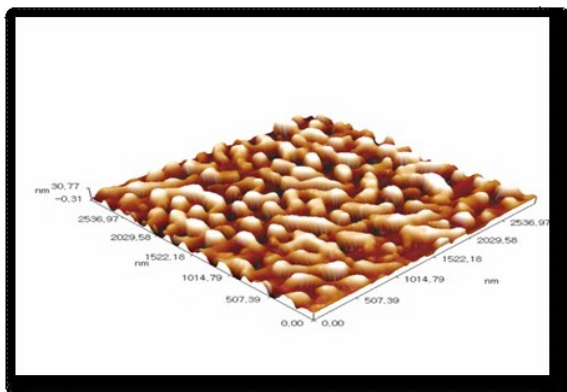


Figure 16. 3-D shape of sample (P).

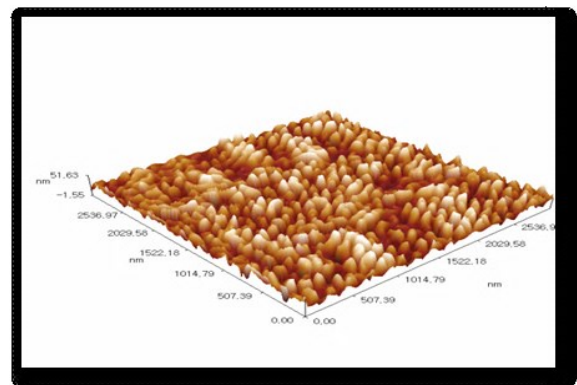


Figure 17. 3-D shape of sample (N).

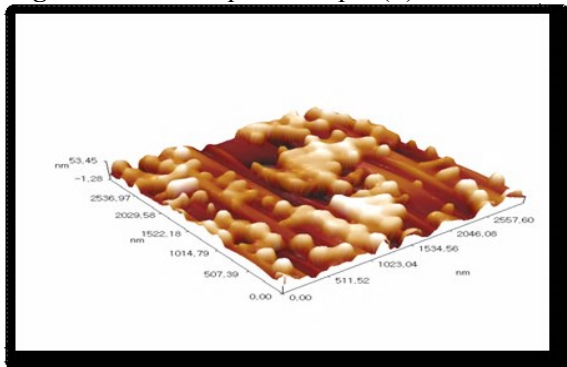


Figure 18. 3-D shape of sample (C).

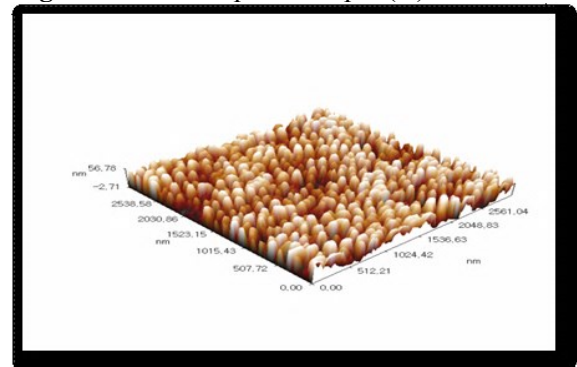


Figure 19. 3-D shape of sample (T).

Figure (20) displays the value of the specimen roughness alloy samples (Ti-Pure, Ti-45%Ni, Ti-10%Co and Ti-30%Ta) after pack cementation deposition with ( $ZrO_2$  and  $Y_2O_3$ ). Depositing and representations of the 3-D shape "topography" of the specimen surface were found to be of big resolution as in Figures (21, 22, 23, and 24). Surface roughness of the samples (P1, N1, C1 and T1) have roughness of (4.2, 3.71, 4.51 and 4.9 nm) respectively. From the roughness values obtained from the atomic force microscopy (AFM), it was found that there are large changes in the roughness value of the samples after depositing as the surface was filled by Nano ceramic material deposition.

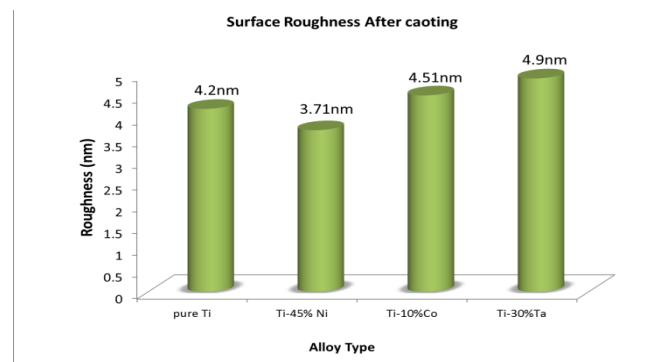


Figure 20. Surface roughness after deposition.

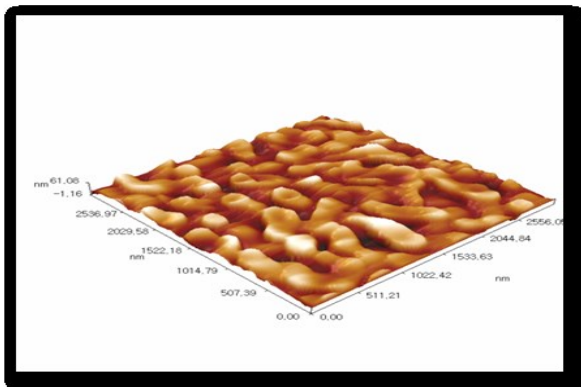


Figure 21. 3-D shape of sample (P1).

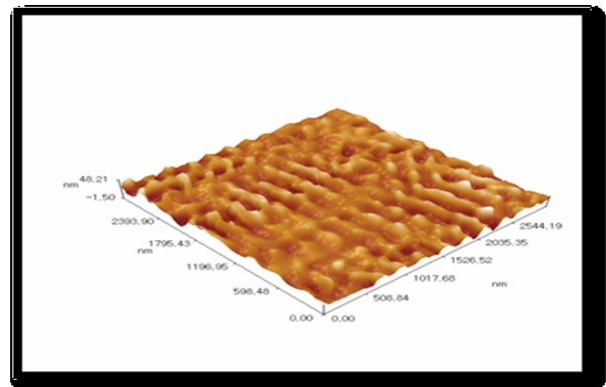


Figure 22. 3-D shape of sample (N1).

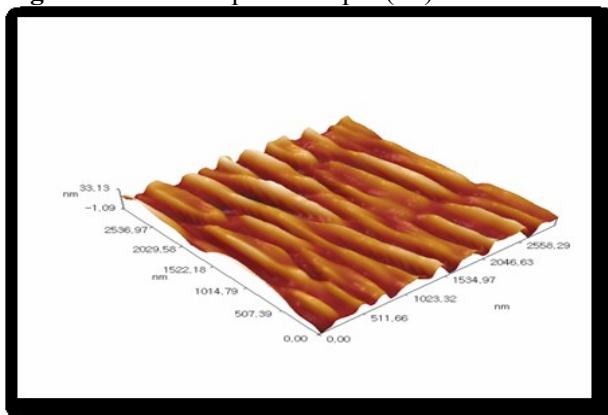


Figure 23. 3-D shape of sample (C1).

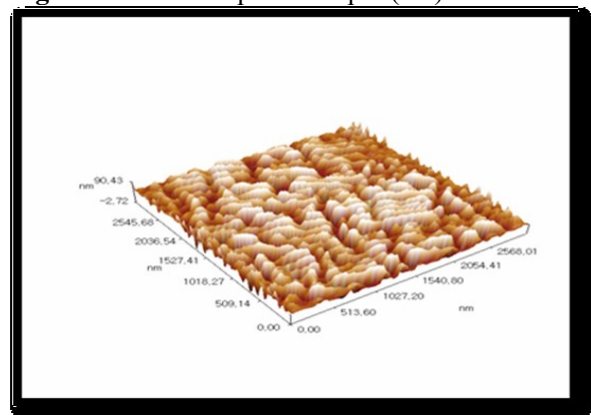
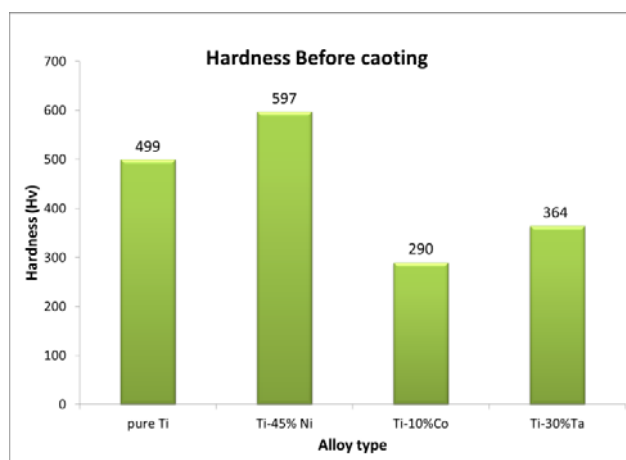


Figure 24. 3-D shape of sample (T1).

### 3.4. Hardness test

The test of hardness was done by taking the average of 5 readings. The results obtained before depositing are represented graphically in figure (25). In this figure, high hardness value was found in sample (N) while lower hardness value was found in sample (C) due to the high porosity percentage that may result in reduced hardness. Hardness tests were made on master sample and these values will be compared with those of the samples after pack cementation deposition with ( $ZrO_2$  and  $Y_2O_3$ ). From figure (26), there was considerable increasing in hardness value. The increase in hardness may be attributed to pores that were coated by material, and the hardness became convergent in value which means that the coating on the surface is homogenous. The other reason to increase hardness can be attributed to the fact that the deposition materials of ceramic have higher hardness than metal.



**Figure 25.** Hardness before deposition.

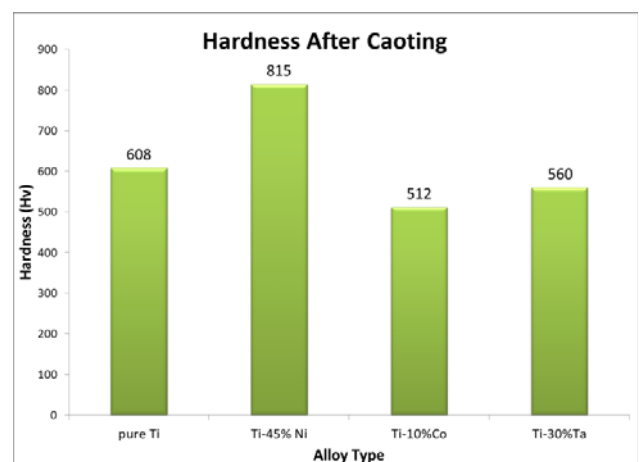


**Figure 26.** Hardness after deposition.

### 3.5. X-Ray Diffractions (XRD)

The XRD exam was conducted using X-ray diffract of Shimadzu meter type (6000) operating at 40.1 kV and 30.1 mA with Cu  $k\alpha$  radiation. The purpose was to find out the structure and identify phases of all specimens. Diffraction of X-ray tests were made for each specimen after the process of sintering and deposition. The diffraction patterns obtained for the samples were the phases that developed as a result of both sintering and deposition which could be detected. Figure (27) displays the pure titanium alloy with single  $\alpha$  phase. There were likely no existence of pure metals that prove the time and temperature of sintering utilized in this work resulting in full sintering reactions. Figures (28), (29), and (30) illustrate the XRD patterns of different titanium alloy before deposition. Figure (28) includes the XRD pattern of sample (P), comprising metallic compound  $Ti_2Co$  in addition to  $\alpha$ -Ti phase. Whereas figure (29) shows the XRD pattern of sample (C), it was noted that the addition of nickel lead to form an intermetallic compound ( $Ni_2Ti_3$ ) in addition to the  $\alpha$ -Ti phase due to the titanium – nickel phase diagram. Figure (30) shows the effect of XRD pattern of sample (T). From this figure, the  $\beta$  second phase appeared in addition to the titanium phases. Only (Ti-30 %Ta) has 2 phases ( $\alpha + \beta$ ) of biphasic structure of XRD patterns.

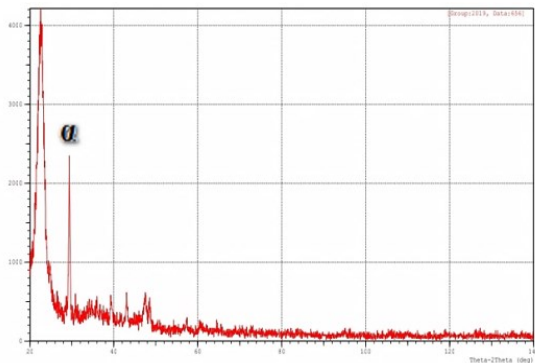


Figure 27. XRD pattern of sample (P).

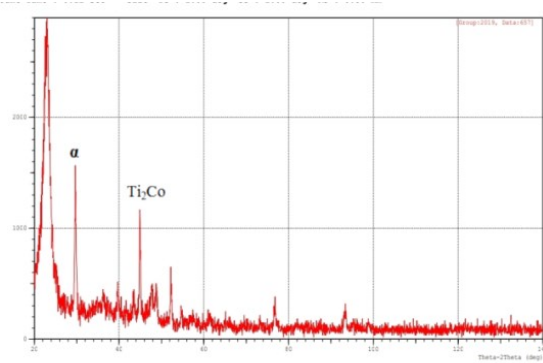


Figure 28. XRD pattern of sample (C).

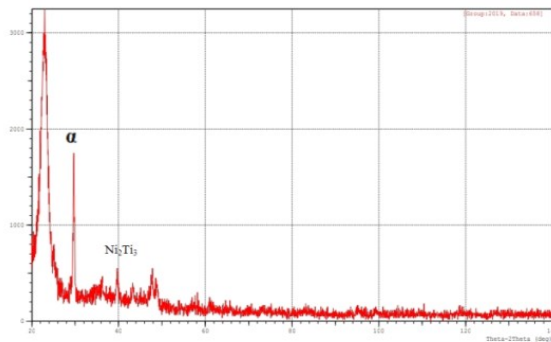


Figure 29. XRD pattern of sample (N).

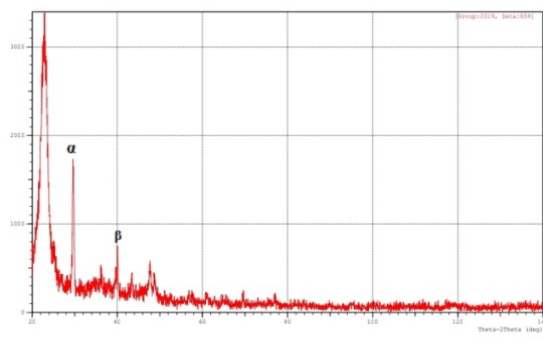


Figure 30. XRD pattern of sample (T).

Figures (31), (32), (33), (34) illustrate the XRD patterns of samples after ( $ZrO_2$  and  $Y_2O_3$ ) deposition by pack cementation process. It was obvious that the amorphous behavior was observed in the XRD after deposition nearly at  $2\theta$  (15.799) for all samples. The peaks in the XRD pattern for titanium alloys match the diffraction angles of  $\alpha$  titanium well. Yet, in ( $ZrO_2$  and  $Y_2O_3$ ) deposition, the peaks slightly shifted to the low angle side. There was no indication that other phases were included in any of the present diffraction patterns. By comparison between XRD patterns at alloys before and after ( $ZrO_2$  and  $Y_2O_3$ ) deposition, it was clear that the pack cementation process was suitable in creation of different surface compositions for all types of Ti-base alloys used.

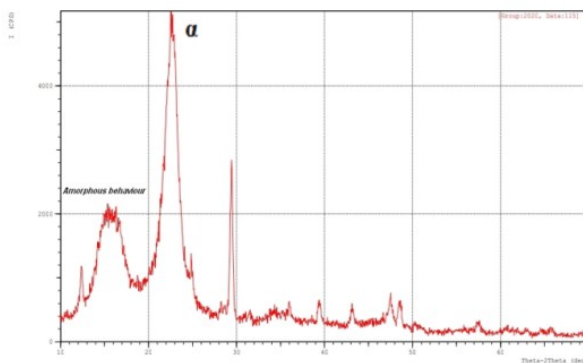


Figure 31. XRD pattern of sample (P1).

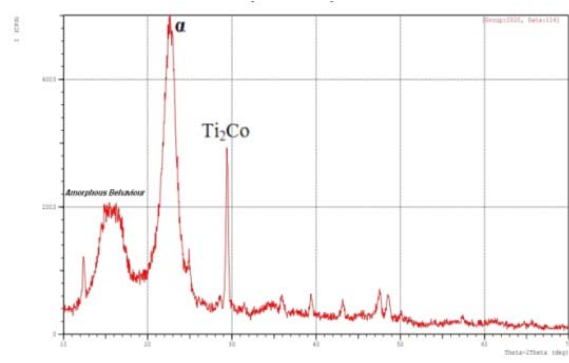
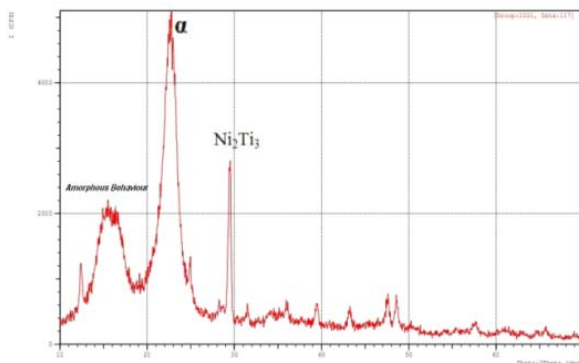
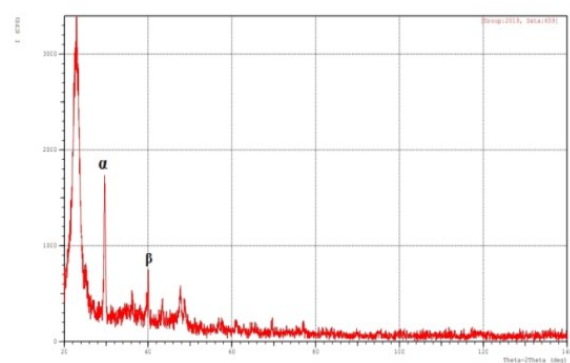


Figure 32. XRD pattern of sample (C1).



**Figure 33.** XRD pattern of sample (N1).



**Figure 34.** XRD pattern of sample (T1).

#### 4. CONCLUSION

According to the results obtained from the current investigation, the following conclusions can be pointed out:

1. Employment of pretreatment surface activation process as chemical acid alkaline etching produces initial surface roughness that increases the efficiency of deposition process.
2. The use of pack cementation as Nano ceramic deposition process results in the formation of Nano zirconia and yttria layer on the surface.
3. The porosity percentage of the samples after Nano ceramic deposition largely decreases due to filling the pores by deposition material.
4. From hardness test, there is considerable increase in hardness value after pack cementation process which may be attributed to pores being filled by Nano ceramic materials.
5. For AFM roughness, it is found that there are large changes in the roughness value of samples after deposition.
6. The peaks in the XRD pattern for titanium alloys match the diffraction angles of titanium well. But after pack cementation process, the peaks slightly shift to the low angle side. Also, amorphous behavior observed in the XRD after deposition is nearly at  $2\theta$  (15.799) for all samples, There was no indication that other phases are included in any of the present diffraction patterns of samples after ( $ZrO_2$  and  $Y_2O_3$ ) deposition.
7. From the SEM, all samples show that Nano zirconia and yttria were homogeneously distributed on the surface and completely covered resulting in significant change in surface morphologies.

#### 5. References

- [1] Stadlinger, Ferguson B, Eckelt S J, Mai U, Lode R, Loukota A T and Slotting R 2012 *Biomechanical Evaluation of a Titanium Implant Surface Conditioned by a Hydrox- Ide Ion Solution* (British Journal of Oral & Maxillofacial Surgery) vol 50 pp 74–79
- [2] Liua X, Chub P K and Dinga C 2004 *Surface Modification Of Titanium, Titanium Alloys, And Related Materials For Biomedical Applications* (Materials Science and Engineering) vol 47 pp 49–121
- [3] Ozcan M and Hammerle C 2012 *Titanium as a Reconstruction and Implant Material in Dentistry: Advantages and Pitfalls* (materials) vol 5 pp 1528–1545
- [4] Batalu D and Liu X 2014 *A Review on Tini Shape Memory Alloys (SMA) used for Medical Applications* (Recycling aspects, Research Gate)
- [5] Machado L G and Savi M A 2003 *Medical Applications of Shape Memory Alloys* (Brazilian Journal

- of Medical and Biological Research) vol 36 pp 683–691
- [6] Straumal B, Korneva A, Kilmametov A R and Lityńska L 2019 *Structural and Mechanical Properties of Ti–Co Alloys Treated by High Pressure Torsion* (materials) vol 12 p 426
- [7] Pang X Z, Hu J and Zhan Y Z 2013 *Microstructural Characteristics of Ti-Co Alloys for Biomedical Applications* (Advanced Materials Research) pp 791–793 pp 469–473
- [8] Capellato P, Riedel N A, Williams J D, Machado J P B, Popat K C and Claro A P R 2013 *Surface Modification on Ti-30Ta Alloy for Biomedical Application* (Engineering) vol 5 pp 707–713
- [9] Das K and Das S 2005 *A Review of the Ti-Al-Ta (Titanium-Aluminum-Tantalum) System* (Phase Equilibria and Diffusion) vol 26 pp 322–329
- [10] Maminskas J, Pilipavicius J, Stasiunas E and Baranovas G 2020 *Novel Yttria-Stabilized Zirconium Oxide and Lithium Disilicate Coatings on Titanium Alloy Substrate for Implant Abutments and Biomedical Application* (Materials) vol 13 p 2070
- [11] Gautam C, Joyner J, Gautam A, Raoc J and Vajtaia R 2016 *Zirconia Based Dental Ceramics: Structure, Mechanical Properties, Biocompatibility And Applications* (Dalton Transaction)
- [12] Asadikiya M, Sabarou H, Chenc M and Zhongab Y 2016 *Phase Diagram For A Nano-Yttria-Stabilized Zirconia System* (RSC Advances) vol 6 pp 17438–17445
- [13] Chen Y W, Moussi J, Drury J L and Wataha J C 2016 *Zirconia In Biomedical Applications* (Expert Review of Medical Devices) vol 13 pp 945–963
- [14] Fatima A H 2019 *Studying the Effect of Cobalt Percentage on the Corrosion Rate of Sintered Titanium Dental Implants* (Technologies and Materials for Renewable Energy, Environment and Sustainability) p 2190
- [15] Gaetano M, Filomena I, Fabio S, Jose C S, Antonino S and Gianrico S 2019 *Effect of Different Surface Treatments on Titanium Dental Implant Micro-Morphology* (Materials)
- [16] Fatima A H 2020 *The Investigation of Ultrasonic Assisted Zirconia Coated Cp–Ti Alloys for Dental Implantation* (Advanced Science and Technology) vol 29 pp 1136–1143
- [17] Wulin H, Xing Y, Li X, Zeping L, Jingtao L, Shujuan Z and Jianwei C 2019 *Enhancing Osseointegration of Titanium Implants Through Large-Grit Sandblasting Combined with Micro-Arc Oxidation Surface Modification* (Materials Science: Materials in Medicine)
- [18] Fatimah J Al-Hasani 2020 *Evaluation of Surface Roughness and Biological Behavior of Ti-Nb Alloys* (Journal of Mechanical Engineering Research and Developments) vol 43 no 7 pp 233-241
- [19] Fatimah J Al-Hasani 2020 *Effect of Cobalt Addition on the Cytotoxicity and Cell Attachment of Titanium Alloys* (Systematic Reviews in Pharmacy) vol 11 no 5
- [20] Rasha A H 2011 *Preparation and Characterization of NiTi Shape Memory Alloys* (MSc thesis, University of Technology, Materials Engineering Department)

### Acknowledgement

I would like to express my gratitude and appreciation to my supervisors Dr. Fatimah J. Al-Hasani for offering me the continuous guidance and encouragement throughout the period of this work. Also, the staff of materials laboratories at the Materials Engineering Department, University of Technology for their great efforts. Deep thanks and appreciation go to my family and friends for their great patience and encouragement throughout the period of.